In Vivo Quantitative Evaluation of the Rat Retinal Nerve Fiber Layer with Optical Coherence Tomography

Atsushi Nagata, Tomomi Higashide, Shinji Ohkubo, Hisashi Takeda, and Kazuhisa Sugiyama

Purpose. To determine whether optical coherence tomography (OCT) is useful for quantitative evaluation of the thickness of the rat retinal nerve fiber layer (RNFL) in an optic nerve crush model.

Methods. An OCT system was developed with a modified commercial time-domain OCT and a superluminescent diode with a bandwidth of 150 nm. Optical components were optimized to acquire rat retinal images. The right optic nerve was crushed intraorbitally with a clip. The left eye served as the untreated control. Circumpapillary OCT scans with a circle diameter of 500 μm centered on the optic disc were performed before and 1, 2, and 4 weeks after the crush. Repeatability and reproducibility of RNFL thickness measurements were evaluated. The RNFL thicknesses at 400, 500, and 600 μm from the center of the optic disc determined by linear vertical OCT scans were compared with thicknesses in retinal sections.

Results. The mean RNFL thicknesses in circumpapillary OCT scans were 27.9 $\pm$ 1.8, 29.2 $\pm$ 2.4, 19.9 $\pm$ 2.3, and 4.5 $\pm$ 3.6 μm before and 1, 2, and 4 weeks after the crush, respectively. RNFL thickness was unchanged 1 week after the crush, but then decreased significantly and progressively after the second week ($P < 0.01$). Coefficients of repeatability and reproducibility were less than 10% except for the crushed eyes at 4 weeks. RNFL thicknesses in OCT images correlated significantly with thicknesses determined histologically ($r = 0.90$, $P < 0.001$).

Conclusions. OCT is a useful and valuable tool for quantitative evaluation of rat RNFL thickness. (*Invest Ophthalmol Vis Sci.* 2009;50:2809–2815) DOI:10.1167/iovs.08-2764

Ocular hypertension, ischemia–reperfusion, and optic nerve crush rodent models have been used to elucidate the pathophysiology of glaucoma and other optic neuropathies.[1,2] In these models, loss of retinal ganglion cells (RGCs) has usually been evaluated histologically by counting the number of cell bodies in the retina or their axons in the optic nerve.[3–6] For intraretinal axons of RGCs, qualitative assessment of the effects of axotomy has been performed by staining the axons in the flatmount retina.[4,7] Recently, we reported on in vivo evaluation of changes in the retinal nerve fiber layer (RNFL) with a scanning laser ophthalmoscope (SLO) in a rat model of optic nerve injury.[8]

Optical coherence tomography (OCT) is a technology capable of producing high-resolution optical cross sections of the retina and providing quantitative measurements of RNFL thickness, macular retinal thickness, and optic disc morphology in human eyes.[9,10] OCT has been also used for imaging the rodent retina.[11–18] However, a MedLine search did not find any reports on OCT evaluation of RNFL changes in rodent eyes with optic nerve injuries, although one study used an OCT for assessing RNFL thickness in normal rat eyes.[15] In this study, we investigated whether OCT is useful for in vivo imaging and quantitative evaluation of rat RNFL in an optic nerve crush model.

Materials and Methods

Animals

Male Brown-Norway rats, 8 weeks of age and weighing 200 to 250 g, were used in the study. The rats had free access to food and water and were maintained in cages in an environmentally controlled room with a 12 hour light–dark cycle. All animals were treated in accordance with the ARVO Statement for the Use of Animals in Ophthalmic and Vision Research. Experimental procedures were approved by the Committee on Animal Experimentation of Kanazawa University (Takara-machi Campus, Japan). All experiments were conducted on rats anesthetized by an intraperitoneal injection (65 mg/kg) of pentobarbital sodium (Somnopentil; Schering-Plough Animal Health, Omaha, NE). For the optic nerve crush model, the optic nerve of the right eye was crushed intraorbitally with a clip (Micro Vascular Clip; Roboz Surgical Instrument Co., Gaithersburg, MD) as described in previous reports.[8,19] The left eye served as the untreated control.

Modification of a Time-Domain OCT for Rat Retina

The quality of images obtained by a commercially available time-domain OCT (EG Scanner; Microtomography Co. Ltd., Yamagata, Japan) was not adequate for visualization of the rat RNFL (Fig. 1A). Given that the coherence length that determines the axial resolution of the OCT system is inversely proportional to the bandwidth,[10] an experimental OCT system was developed with the time-domain OCT and a multiplexed two-superluminescent-diode (SLD) light source (Broadlighter; Superlum Diodes, Ltd., Moscow, Russia). The SLD had a center wavelength of 890 nm, a bandwidth of 150 nm, and an output power of 6 mW, whereas the original SLD had a center wavelength of 830 nm, a bandwidth of 20 nm, and an output power of 6 mW.

Optical components (beam splitter, mirror, and lens) in the experimental OCT system were optimized for the new SLD. To improve the signal-to-noise ratio, which decreases with a broader bandwidth SLD, the signal frequency was changed from 15 to 5 MHz. The resultant image acquisition time was lengthened from 1.5 to 4.5 seconds. Along with these modifications, the filter property in the analog signal processor was optimized to the high-resolution signal produced by the broadband light source. A dispersion compensating glass block was inserted in the reference arm to correct the dispersion imbalance

From the Department of Ophthalmology and Visual Science, Kanazawa University Graduate School of Medical Science, Kanazawa, Japan.

Supported by Grant-in-Aid for Scientific Research 20592035 from the Japanese Society for the Promotion of Science.

Submitted for publication August 23, 2008; revised November 25, 2008, and January 7, 2009; accepted April 9, 2009.

Disclosure: **A. Nagata**, None; **T. Higashide**, None; **S. Ohkubo**, None; **H. Takeda**, None; **K. Sugiyama**, None

The publication costs of this article were defrayed in part by page charge payment. This article must therefore be marked "*advertisement*" in accordance with 18 U.S.C. §1734 solely to indicate this fact.

Corresponding author: Tomomi Higashide, Department of Ophthalmology and Visual Science, Kanazawa University Graduate School of Medical Science, 13-1 Takara-machi, Kanazawa 920-8641, Japan; eyetomo@kenroku.kanazawa-u.ac.jp.

between the sample and reference arms of the interferometer, which was caused by the change in SLD bandwidth. In addition, the light path length was modified to be suitable for rat eyes with a short axial length. The power delivered to the rat eye was 1200 μW. Each scan consisted of 600 axial scans (133 axial scans per second). Each axial scan sampled 1600 axial pixels spanning an axial range of 1.0 mm. The calibrated axial resolution of the system was 5.8 μm in air, corresponding to 4.3 μm in tissue, which was significantly improved compared with that of the original SLD (10–20 μm in tissue). The measured system sensitivity was 80 dB. The dynamic range of the OCT images was 30 dB.

According to data of representative rat[20] and human (Gullstrand's schematic eye) eyes, the total power of the rat eye is much greater than that of the human eye (300.705 vs. 58.64 D). Therefore, lateral magnification of the rat fundus should be approximately five times larger than that of the human fundus. Accordingly, the imaging area of the charge-coupled device (CCD) camera, which displayed the fundus and the scan positions, was approximately 2×2 mm^2 in rat eyes compared with 1×1 cm^2 in human eyes.

OCT Imaging of Rat RNFL

OCT imaging of RNFL in rat eyes was performed before (baseline) and at 1, 2, and 4 weeks after optic nerve crush ($n = 9$). The eyes were dilated with 0.5% tropicamide and 0.5% phenylephrine hydrochloride eye drops (Santen Pharmaceuticals, Osaka, Japan). To preserve corneal clarity throughout the experiment, a custom-made contact lens with a radius of curvature of 2.75 mm, a diameter of 5.0 mm, and 0 D (Unicon Corp., Osaka, Japan) was placed on the cornea after topical anesthesia with 0.4% oxybuprocaine hydrochloride eye drops (Santen Pharmaceuticals). The rat was placed on a platform without any fixation of the head or eye. The platform could be rotated manually around the longitudinal axis of the body or in the horizontal plane. This facilitated careful adjustment of the eye position to keep the optic disc in the center of the CCD camera image and the scan beam perpendicular to the fundus. Although our time-domain OCT takes considerable time for a single scan (4.5 seconds), rats under general anesthesia did not cause significant motion problems of the head or eye during the scan. Circumpapillary OCT scans with a circle diameter of 500 μm centered on the optic disc were performed at each time point (four OCT sessions during the experimental period).

To compare RNFL thickness determined by OCT images and histology, we also performed vertical linear OCT scans at distances of 400, 500, and 600 μm from the center of the optic disc (toward the temporal or nasal side in the right or left eye, respectively) at 4 weeks after the crush followed by histologic preparations. Linear scan data of all nine right eyes and five left eyes were treated as data at 4 weeks after the crush and baseline, respectively. The right eyes of additional rats were used for linear scans and histologic evaluation at 1 and 2 weeks after the crush ($n = 3$ and 5, respectively).

For both circumpapillary and linear OCT scans, three scans with good image quality were recorded for each eye at each time point. RNFL thicknesses were measured manually in each of three OCT scans with image-analysis software (Image-Pro Plus 6.0; MediaCybernetics, Inc., Silver Spring, MD) in a masked fashion by a single observer, and the mean thickness was determined. In areas where a major blood vessel interrupted RNFL tissue, the RNFL thickness was determined as the average of the RNFL thickness measurements from the two adjacent points.[21]

Histologic Evaluation of the Rat RNFL

Immediately after linear OCT scan imaging, the rats were given an overdose of anesthesia and perfused through the left ventricle first with saline, then with 4% paraformaldehyde-0.5% glutaraldehyde in 0.1 M phosphate buffer. The eyes were enucleated, the anterior segment of each eye was removed; and a small marking cut was placed on the edge of the posterior eye cup to identify the superior retinal portion. The eye cup was fixed in 4% paraformaldehyde-0.5% glutaraldehyde in 0.1 M phosphate-buffered saline for 2 hours at room temperature and was embedded in paraffin. Serial 6-μm paraffin-embedded sections were cut along the vertical meridian of the globe. The section number (*Ny*) corresponding to a certain distance (*Y*) from the center of the optic disc in the CCD camera image was estimated from the total number of sections that were cut through the optic disc (*Nd*) and the diameter of the optic disc in the CCD camera image (*D*) as follows: $Ny = Nd \times Y/D$. Retinal sections taken from locations 400, 500, and 600 μm distant from the center of the optic disc (corresponding the locations of linear OCT scans) were stained with hematoxylin-eosin and observed under an optical microscope (Axioplan2; Carl Zeiss Jena GmbH, Jena, Germany). The digital images were recorded as JPEG files with a digital cooled CCD camera (DS-5Mc-L1; Nikon Corp., Kanagawa, Japan). For each eye, RNFL thickness in each retinal section was measured with image-analysis software (Image-Pro Plus 6.0; Media Cybernetics) in a masked fashion by a single observer. In areas in which a major blood vessel interrupted RNFL tissue, the RNFL thickness was determined as described previously for OCT imaging.

Statistical Analysis

Differences in RNFL thickness were analyzed by paired *t*-tests for comparisons between control and crushed eyes or OCT images and retinal sections and by repeated-measures ANOVA and post hoc analyses for comparisons between different time points, different quadrants, or different retinal locations in the same retina. Differences in the superior/inferior and temporal/nasal ratios of RNFL thickness at different time points were analyzed by the Friedman test. Pearson's correlation coefficient was used to test the correlations between RNFL thicknesses determined from OCT images and from retinal sections. $P < 0.05$ was considered statistically significant. Data are expressed as the mean ± SD.

To examine the repeatability and reproducibility of RNFL thickness measurements by OCT, the coefficient of repeatability ($1.96 \times$ SD of differences between pairs of measurements in the same eye during the same OCT session) and the coefficient of reproducibility ($1.96 \times$ SD of differences between measurements in the same eye at different OCT sessions) were calculated according to methods outlined by Bland and Altman.[22–24] The coefficient of repeatability was determined by using RNFL thickness measurements in two of three circumpapillary scans (first and third scans) in the same eye during the same OCT session. The coefficient of reproducibility was determined by using mean RNFL thickness measurements in circumpapillary scans in the same control eye at different OCT sessions. Coefficients of repeatability and reproducibility were also expressed as a percentage of the mean measurement (this is equal to $1.96 \times$ coefficient of variation).[24]

Results

OCT Imaging of Rat RNFL

OCT images obtained with commercial time-domain OCT showed only that the rat retina had two layers, with strong refraction from the inner layer and weak refraction from the outer layer, and the images were not clear enough to identify the RNFL (Fig. 1A). By contrast, the rat RNFL was clearly visualized with the experimental OCT (Fig. 1B). Furthermore, comparisons between the retinal section (Fig. 1C) corresponding with the location of the OCT scan and the OCT image (Fig. 1D) clearly demonstrated that other retinal layers were also discernible in the OCT image.

RNFL Changes in Thickness over Time Caused by the Optic Nerve Crush

Mean RNFL thicknesses measured in circumpapillary OCT scans with a circle diameter of 500 μm centered on the optic disc were 27.9 ± 1.8, 29.2 ± 2.4, 19.9 ± 2.3, and 4.5 ± 3.6 μm at baseline and 1, 2, and 4 weeks after the optic nerve crush,

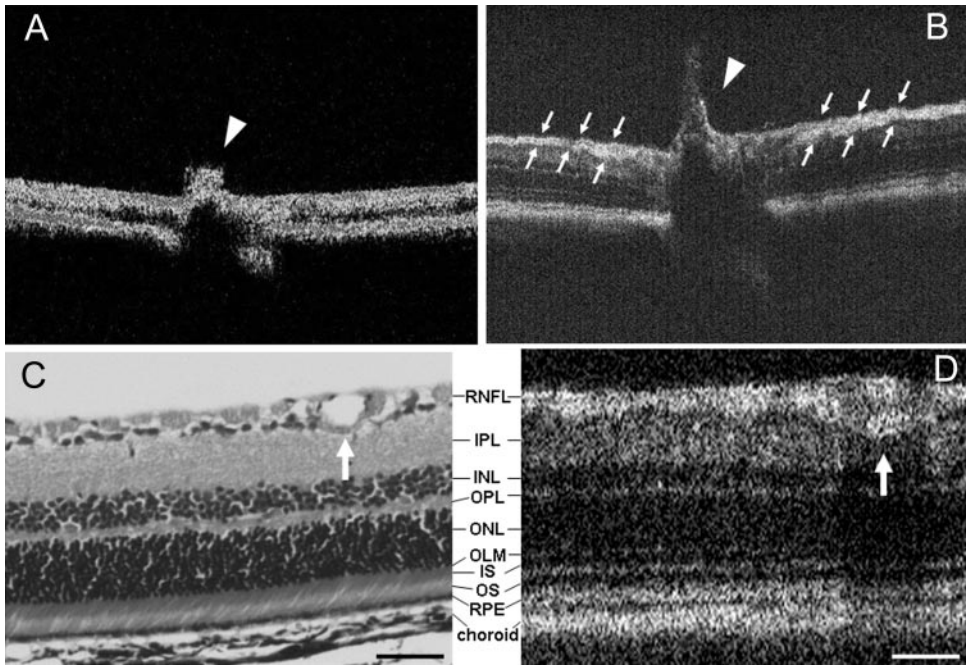

FIGURE 1. Improvement of axial resolution by broad-bandwidth SLD in OCT images of rat retina. (**A**) OCT image by commercially available time-domain OCT. (**B**, **D**) OCT image by the modified OCT with a broad-bandwidth SLD. (**C**) Retinal section stained with hematoxylin-eosin at the retinal location corresponding to the OCT image in (**D**). (**A**, **B**, *arrowheads*) optic nerve head; (**B**, *arrows*) RNFL; (**C**, **D**, *arrows*) major blood vessel. Scale bar, 50 μm.

respectively (Figs. 2, 3). RNFL thickness was unchanged 1 week after the crush, but then decreased significantly and progressively after the second week ($P < 0.01$). There were no significant changes in RNFL thickness in the untreated control eyes during the experimental period (Fig. 3). To compare normal RNFL thickness by quadrants, we combined baseline OCT data from both eyes. The mean RNFL thickness was 29.6 ± 4.1, 27.5 ± 3.4, 27.9 ± 3.9, and 26.1 ± 2.3 μm in the superior, temporal, nasal, and inferior quadrants, respectively. The mean RNFL thickness measured in the superior quadrant was significantly greater than the mean thickness in the inferior quadrant ($P < 0.05$). The RNFL changes in thickness in each quadrant, caused by the optic nerve crush, are shown in Figure 4. There were no significant differences in RNFL thickness changes among the different quadrants 1 and 2 weeks after the optic nerve crush. However, RNFL thickness in the inferior quadrant was significantly greater than thickness in the temporal and nasal quadrants 4 weeks after the crush ($P < 0.01$), although the difference was less than 10%.

Superior/inferior and temporal/nasal ratios of RNFL thickness were also examined at each time point. Superior/inferior ratios, expressed as a percentage of the baseline value (100% ± 9.8%), were 95.6% ± 9.1%, 88.1% ± 10.5%, and 86.4% ± 32.5% at 1, 2, and 4 weeks after the optic nerve crush, respectively.

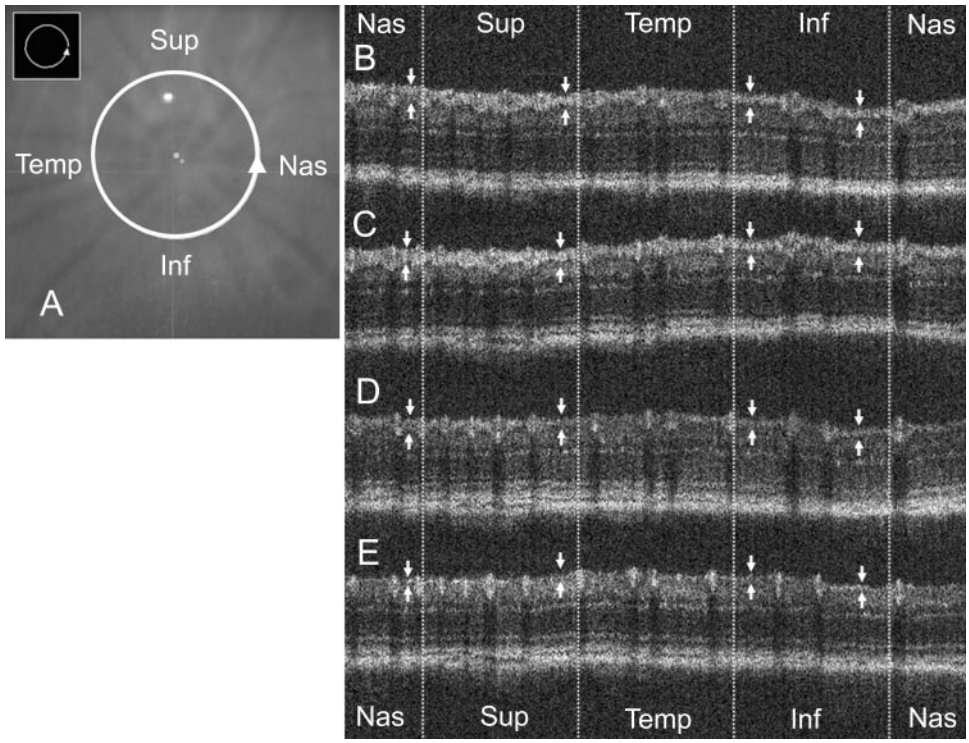

FIGURE 2. RNFL changes over time caused by optic nerve crush. (**A**) Fundus image by CCD camera, with a scan circle with a diameter of 500 μm centered on the optic disc. *Arrow*: scan direction. Circumpapillary OCT images at baseline (**B**) and 1 (**C**), 2 (**D**), and 4 (**E**) weeks after the crush. (**B**–**E**, *arrows*) RNFL. Nas, nasal quadrant; Sup, superior quadrant; Temp, temporal quadrant; Inf, inferior quadrant.

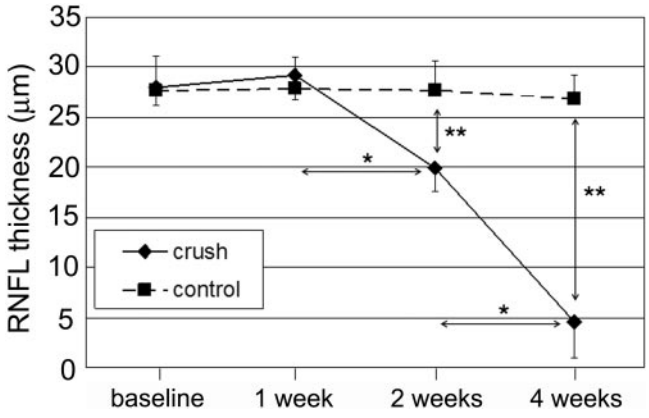

FIGURE 3. Changes in mean RNFL thickness in circumpapillary OCT scans caused by optic nerve crush. Data are presented as the mean ± SD ($n = 9$ each). $^{*}P < 0.01$ (repeated-measures ANOVA). $^{**}P < 0.001$ (paired *t*-test).

Similarly, temporal/nasal ratios, also expressed as a percentage of the baseline value (100% ± 14.5%), were 99.8% ± 10.5%, 96.7% ± 11.0%, and 112.3% ± 84.8% at 1, 2, and 4 weeks after the optic nerve crush, respectively. Neither the superior/inferior nor the temporal/nasal ratio was significantly different across time points.

RNFL Thickness in OCT Images Versus Retinal Sections

To determine whether RNFL thickness in OCT images is a reliable indicator of actual RNFL thickness, RNFL thickness was measured in paraffin-embedded sections corresponding to locations in linear OCT scans. RNFL thicknesses determined by OCT scans had significantly positive correlations with the thicknesses determined by retinal sections, except for the measurements at 4 weeks after the crush (overall, $r = 0.90$, $P < 0.001$; control and 1 week, $r = 0.56$, $P < 0.01$; 2 weeks, $r = 0.80$, $P < 0.001$; and 4 weeks, $r = 0.26$, $P = 0.19$; Fig. 5). We also compared RNFL thicknesses measured in the same control eye at different retinal locations (Fig. 6). RNFL thicknesses in linear OCT scans at locations 400, 500, and 600 μm distant from the center of the optic disc were 34.6 ± 3.6, 27.6 ± 2.2, and 25.2 ± 4.4 μm, respectively, compared with

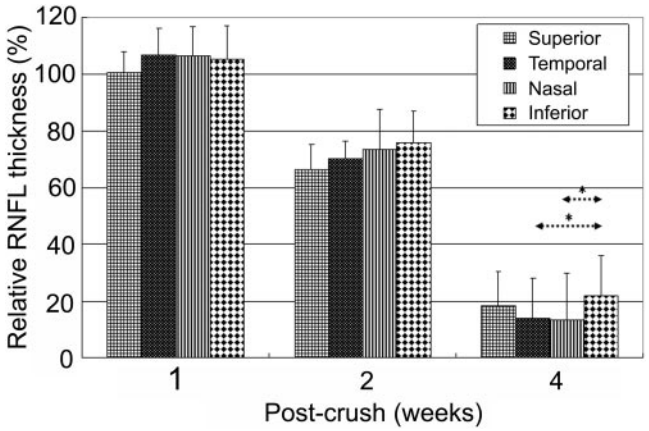

FIGURE 4. Changes in RNFL thickness in each quadrant caused by optic nerve crush. RNFL thickness after the crush is expressed as the percentage of the baseline value in each quadrant. Data are presented as the mean ± SD ($n = 9$ each). $^{*}P < 0.01$ (repeated-measures ANOVA).

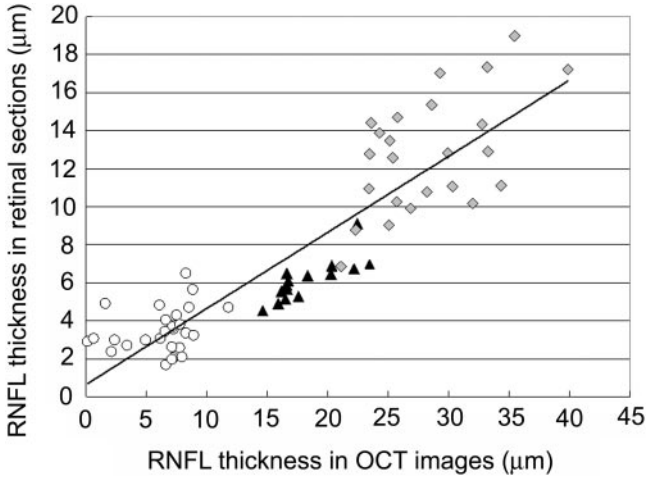

FIGURE 5. Correlation of RNFL thickness determined by OCT and histology. Pearson's correlation coefficient analysis shows a significantly positive relationship between OCT and histologically determined RNFL thickness, except at 4 weeks after the crush (overall, $r = 0.90$, $P < 0.001$; control and 1 week, $r = 0.56$, $P < 0.01$; 2 weeks, $r = 0.80$, $P < 0.001$; 4 weeks, $r = 0.26$, $P = 0.19$). *Diamonds*: control and 1 week; *triangles*: 2 weeks; *circles*: 4 weeks.

corresponding retinal sections of 15.5 ± 3.4, 12.2 ± 2.7, and 10.0 ± 2.8 μm, respectively. RNFL thicknesses in the OCT images were significantly thicker than those determined in retinal sections ($P < 0.001$, 400 and 500 μm; $P < 0.01$, 600 μm). RNFL thicknesses in both OCT images and retinal sections decreased significantly with lengthening distance from the center of the optic disc ($P < 0.01$, 400 vs. 500 μm; $P < 0.05$, 500 vs. 600 μm in both OCT and histologic measurements).

Repeatability and Reproducibility of RNFL Thickness Measurements by OCT

The coefficient of repeatability was less than or equal to 2.5 μm in both crushed and control eyes at all experimental time points (Table 1). When expressed as a percentage of the mean measurement, the coefficient of repeatability was less than 10% except for that of the crushed eyes at 4 weeks (51.9%). The coefficient of reproducibility was less than 2.5 μm or 10% in control eyes during the experimental period (Table 2).

Discussion

We developed an OCT for rat fundus from a commercially available time-domain OCT and successfully evaluated rat RNFL-thickness changes over time in an optic nerve crush model. Recently, Kawaguchi et al.[8] reported on the in vivo evaluation of rat RNFL thickness with SLO. Although the RNFL thicknesses estimated by SLO correlated well with thicknesses determined by histology, the method could neither show the cross-sectional images of RNFL nor determine the absolute thickness. Because of this, OCT is more suitable than SLO for RNFL thickness measurements. However, OCT imaging of the rodent fundus has been challenging because the rodent eye is small, with a short focal length. In previous studies, time-domain OCT of rodent eyes has been reported to be useful in assessing retinal degeneration,[11,12] choroidal neovascularization,[13] and retinal transplantation.[14] However, the axial resolution of the time-domain OCT used in these studies was not adequate for evaluating RNFL thickness in rodent eyes. To improve the axial resolution, we used a SLD with a broader bandwidth than the built-in SLD, which resulted in visualiza-

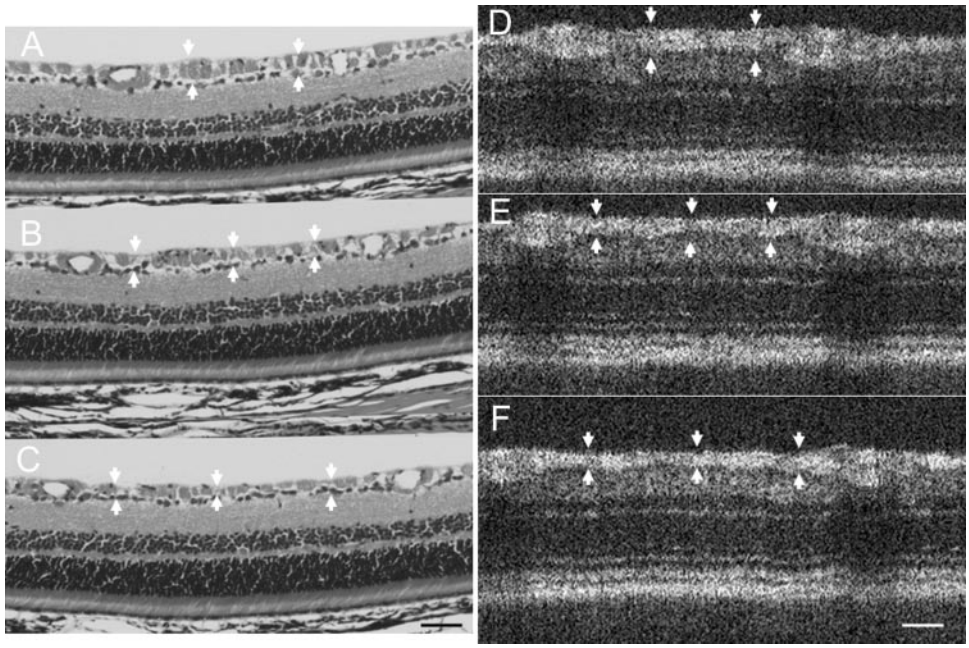

FIGURE 6. Comparison of RNFL thicknesses in the same control eye at different locations. (**A**–**C**) retinal sections; (**D**–**F**) OCT images. Retinal sections were derived from the locations corresponding to OCT images: 400 (**A**, **D**), 500 (**B**, **E**), and 600 (**C**, **F**) μm from the center of the optic disc. *Arrows*: RNFL. Scale bars, 50 μm.

tion of RNFL as well as other retinal layers. The image quality approached that obtained by the recently reported spectral-domain OCT system, which has high-speed and high-resolution imaging.[15,17] Using a spectral-domain OCT, Srinivasan et al.[15] reported that RNFL thickness near the optic disc was approximately 30 μm in normal Long-Evans rats, which is in good agreement with our results. However, the RNFL thickness measured in OCT images was significantly larger than that measured in retinal sections. The discrepancy may be explained by artifacts inherent in histologic preparation, including tissue shrinkage from fixation and compression during sectioning.[25,26]

In normal human eyes, OCT and histologic studies have shown that the peripapillary RNFL thickness has a double-hump pattern with peaks in the superior and inferior quadrants and troughs in the temporal and nasal quadrants.[27,28] Both studies showed that the RNFL thickness in the peak quadrants are at least 40% thicker than thicknesses in the trough quadrants. In contrast, peripapillary RNFL thicknesses in rat eyes were relatively uniform, although RNFL in the superior quadrant is significantly thicker than RNFL in the inferior quadrant by approximately 14%. The superior–inferior difference in RNFL thickness may reflect a difference in the density of RGCs, with the highest density in the superotemporal quadrant[29]; however, in a later study, the findings were not confirmed.[30] Another possibility for the RNFL thickness differences may be artifacts inherent in OCT scanning procedures. A displacement of the scan circle may cause RNFL thickness differences. Given that RNFL thickness decreased in relation to the distance from the center of the optic disc, the scan circle may have been displaced inferiorly, although the scan circle was carefully centered on the optic disc for each CCD camera image during OCT scanning. The perpendicularity of optical sectioning by OCT must be constant along the scan circle. Greater deviation from perpendicularity may result in greater thickness measurements. However, the mean difference at baseline between superior and inferior quadrants in total retinal thickness measured by OCT imaging was less than 2%, indicating that deviation in perpendicularity was not the explanation for the RNFL thickness differences between quadrants (data not shown). The possible regional differences in RNFL thickness in rat eyes deserve further study.

To our knowledge, no studies have reported on the OCT evaluation of RNFL thickness changes in rodent models of optic nerve injuries. The optic nerve crush model is a well-established model for glaucoma and optic neuropathy; it induces RGC loss secondary to the mechanical damage to the axon.[1,2] The time courses and the magnitude of RGC loss after axonal injury are different depending on the site (intracranial versus intraorbital injury) and the severity of the insult (from partial crush to total axotomy).[31–33] Several studies showed that optic nerve injury causes a delayed phase of RGC loss

TABLE 1. Repeatability of Rat RNFL Thickness Measurements by OCT

Circumpapillary Scans	Mean of Scan (1 + 3) (μm)	Mean of ΔScan (1 − 3) (μm)	SD (μm)	CR (1.96 × SD) (μm)	CR (1.96 × SD/Mean) (%)
Crush*: baseline	27.9	0.4	1.3	2.5	9.0
Crush: 1 week	29.1	−0.1	1.1	2.1	7.3
Crush: 2 weeks	19.9	−0.4	0.8	1.6	7.8
Crush: 4 weeks	4.7	0.1	1.3	2.5	51.9
Control†: baseline	27.8	−0.2	1.0	2.0	7.1
Control: 1 week	27.9	−0.2	1.1	2.1	7.7
Control: 2 weeks	27.8	−0.7	0.7	1.4	4.9
Control: 4 weeks	26.9	0.4	0.9	1.8	6.7

* Eyes with optic nerve crush.
† Control eyes.

TABLE 2. Reproducibility of Rat RNFL Thickness Measurements by OCT

Circumpapillary Scans in Control Eyes		Mean of Two Sessions (μm)	Mean Δ of Sessions (1 − 2) (μm)	SD (μm)	CR (1.96 × SD) (μm)	CR (1.96 × SD/mean) (%)
Session 1	Session 2					
Baseline	1 Week	27.8	−0.2	1.1	2.1	7.5
1 Week	2 Weeks	27.8	0.2	1.1	2.2	7.7
2 Weeks	4 Weeks	27.3	0.8	1.2	2.3	8.6

(secondary degeneration) after a rapid phase of cell death due to the primary insult.[34,35] Although RGC loss after optic nerve crush has been examined in several studies, the information regarding the postcrush changes in intraretinal RGC axons is quite limited.[4,7,8] Recently, we reported on the in vivo SLO evaluation of RNFL changes in the rat optic nerve crush model.[8] The range of refractive values in SLO in which the RNFL reflex was clearly observed was unchanged 1 week after the crush, but then decreased significantly and progressively after the second week. In this study, using the same rat model, we used OCT and observed similar RNFL changes over time after the optic nerve crush. The RNFL thickness changes did not differ much by quadrant in this study. These results were also in agreement with the SLO study, which demonstrated the uniform attenuation of RNFL reflex after the crush. In contrast, Higashide et al.[19] reported that the decrease in the RGC counts evaluated in vivo by SLO had already exceeded 50% at 1 week in exactly the same experimental model as this study. Therefore, the reduction of RNFL thickness appeared to be lagging behind the RGC loss. The reason for the dissociation of time courses between loss of intraretinal axons and cell bodies is currently unknown. The clearance processes for intraretinal RGC axons may differ from those for cell bodies. Further studies examining the relationship between RNFL thickness and severity of the crush injury and between RNFL thickness and the number of surviving RGCs will enhance the understanding of the process of retinal nerve fiber loss after optic nerve injury. Also, RNFL thickness measurements at time points earlier than 1 week after injury would be informative regarding acute responses to optic nerve crush injury including tissue edema. However, conjunctival swelling may cause difficulty in obtaining clear OCT images in the early time frame.

In this study, RNFL thickness measurements by OCT had relatively good repeatability and reproducibility (≤2.5 μm) in comparison with measurements in human eyes. The test–retest variability of human RNFL thickness measurements by Stratus OCT was reported to be within 6 μm.[36] However, when expressed as a percentage of the mean measurement, repeatability in this study was poor in crushed eyes at 4 weeks with a mean RNFL thickness of 4.5 μm. Reflecting this result, RNFL thicknesses that were determined by OCT scans had no significant correlation with thicknesses determined by retinal sections at 4 weeks after the crush. The poor repeatability and poor correlation with retinal sections for RNFL thickness less than 5 μm may be explained by the limitation in the axial resolution of the OCT system.

The current OCT system has several areas that need improvement. First, although the repeatability and reproducibility of RNFL thickness measurements were relatively good, the measurements were performed manually because the dynamic range and signal-to-noise ratio of OCT images may not be sufficient to allow computerized segmentation of the retinal layers for automatic measurements. Obviously, manual measurements are time-consuming and likely to involve subjective bias. In this regard, we are trying multiple scan averaging to improve the signal-to-noise ratio.[37] Although our time-domain OCT takes considerable time for a single scan (4.5 seconds), rats under general anesthesia did not cause significant motion problems during the scan. However, for multiple scan averaging, we additionally used a fixation device for the rat's head (Fig. 7B), which successfully maintained stability of the rat fundus for at least several minutes. Preliminary data showed improved image quality by multiple scan averaging (Fig. 7). However, to construct a peripapillary RNFL thickness map instead of a circumpapillary thickness profile with a fixed-diameter scan circle, it is mandatory to use 3D-OCT imaging,[15,17] which is made possible by spectral-domain OCT, which has much faster scanning speed than time-domain OCT.

In conclusion, we developed an OCT for in vivo imaging and quantitative evaluation of rat RNFL from a commercially available time-domain OCT. Evaluation of rat RNFL by OCT will be informative not only in optic nerve crush models but also in other models of optic nerve damage for studying the pathology

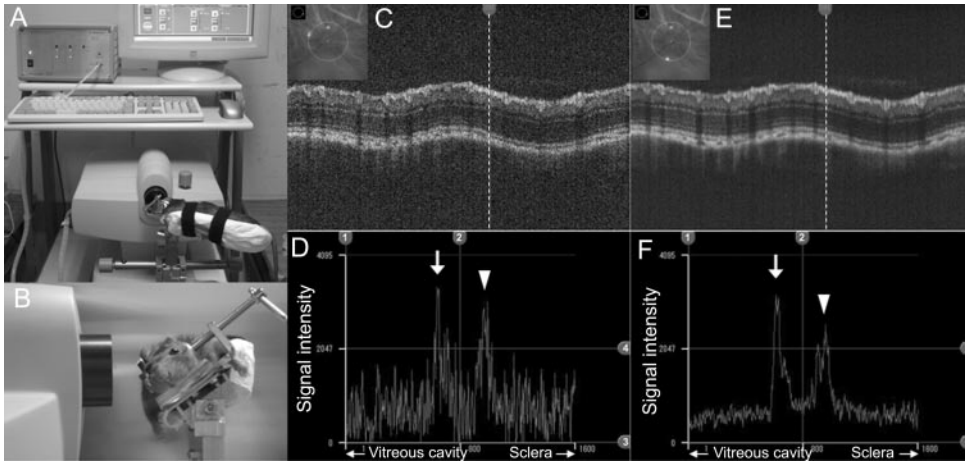

FIGURE 7. Improvement of the OCT image quality by multiple scan averaging (preliminary data). (**A**) Overview of the OCT system; (**B**) higher magnification view of the rat head fixation device; circumpapillary OCT images by a single scan (**C**) and by averaging 10 scans (**E**). (**C**, **E**, *dotted lines*) The positions corresponding to the axial scans in (**D**) and (**F**), respectively. Examples of the axial scan profile in a single scan (**D**) and 10-scan averaging (**F**). Signal-to-noise ratio appears to be improved by multiple scan averaging. (**D**, **F**, *arrows*, *arrowheads*) the positions of RNFL and RPE/choroid, respectively.

of optic neuropathy including glaucoma and for developing new therapies.

Acknowledgments

The authors thank Tohru Nakagawa, Kunio Yashima, and Michiro Hasegawa (Microtomography Co., Ltd., Yamagata, Japan) for technical support.

References

1. Goldblum D, Mittag T. Prospects for relevant glaucoma models with retinal ganglion cell damage in the rodent eye. *Vision Res.* 2002;42:471–478.
2. Pang IH, Clark AF. Rodent models for glaucoma retinopathy and optic neuropathy. *J Glaucoma.* 2007;16:483–505.
3. Allcutt D, Berry M, Sievers J. A quantitative comparison of the reactions of retinal ganglion cells to optic nerve crush in neonatal and adult mice. *Brain Res.* 1984;318:219–230.
4. Villegas-Perez MP, Vidal-Sanz M, Bray GM, Aguayo AJ. Influences of peripheral nerve grafts on the survival and regrowth of axotomized retinal ganglion cells in adult rats. *J Neurosci.* 1988;8:265–280.
5. Chauhan BC, Pan J, Archibald ML, LeVatte TL, Kelly ME, Tremblay F. Effect of intraocular pressure on optic disc topography, electroretinography, and axonal loss in a chronic pressure-induced rat model of optic nerve damage. *Invest Ophthalmol Vis Sci.* 2002; 43:2969–2976.
6. Mabuchi F, Aihara M, Mackey MR, Lindsey JD, Weinreb RN. Optic nerve damage in experimental mouse ocular hypertension. *Invest Ophthalmol Vis Sci.* 2003;44:4321–4330.
7. Allcutt D, Berry M, Sievers J. A qualitative comparison of the reactions of retinal ganglion cell axons to optic nerve crush in neonatal and adult mice. *Brain Res.* 1984;318:231–240.
8. Kawaguchi I, Higashide T, Ohkubo S, Takeda H, Sugiyama K. In vivo imaging and quantitative evaluation of the rat retinal nerve fiber layer using scanning laser ophthalmoscopy. *Invest Ophthalmol Vis Sci.* 2006;47:2911–2916.
9. Chang R, Budenz DL. New developments in optical coherence tomography for glaucoma. *Curr Opin Ophthalmol.* 2008;19:127–135.
10. Costa RA, Skaf M, Melo LA Jr, et al. Retinal assessment using optical coherence tomography. *Prog Retin Eye Res.* 2006;25:325–353.
11. Horio N, Kachi S, Hori K, et al. Progressive change of optical coherence tomography scans in retinal degeneration slow mice. *Arch Ophthalmol.* 2001;119:1329–1332.
12. Li Q, Timmers AM, Hunter K, et al. Noninvasive imaging by optical coherence tomography to monitor retinal degeneration in the mouse. *Invest Ophthalmol Vis Sci.* 2001;42:2981–2989.
13. Fukuchi T, Takahashi K, Shou K, Matsumura M. Optical coherence tomography (OCT) findings in normal retina and laser-induced choroidal neovascularization in rats. *Graefes Arch Clin Exp Ophthalmol.* 2001;239:41–46.
14. Thomas BB, Arai S, Ikai Y, et al. Retinal transplants evaluated by optical coherence tomography in photoreceptor degenerate rats. *J Neurosci Methods.* 2006;151:186–193.
15. Srinivasan VJ, Ko TH, Wojtkowski M, Carvalho M, Clermont A, Bursell SE. Noninvasive volumetric imaging and morphometry of the rodent retina with high-speed, ultrahigh-resolution optical coherence tomography. *Invest Ophthalmol Vis Sci.* 2006;47:5522–5528.
16. Kocaoglu OP, Uhlhorn SR, Hernandez E, et al. Simultaneous fundus imaging and optical coherence tomography of the mouse retina. *Invest Ophthalmol Vis Sci.* 2007;48:1283–1289.
17. Ruggeri M, Wehbe H, Jiao S, et al. In vivo three-dimensional high-resolution imaging of rodent retina with spectral-domain optical coherence tomography. *Invest Ophthalmol Vis Sci.* 2007;48: 1808–1814.
18. Kim KH, Puoris'haag M, Maguluri GN, et al. Monitoring mouse retinal degeneration with high-resolution spectral-domain optical coherence tomography. *J Vision.* 2008;8:17.1–11.
19. Higashide T, Kawaguchi I, Ohkubo S, Takeda H, Sugiyama K. In vivo imaging and counting of rat retinal ganglion cells using a scanning laser ophthalmoscope. *Invest Ophthalmol Vis Sci.* 2006; 47:2943–2950.
20. Hughes A. A schematic eye for the rat. *Vision Res.* 1979;19:569–588.
21. Blumenthal EZ. Quantifying retinal nerve fiber layer thickness histologically: a novel approach to sectioning of the retina. *Invest Ophthalmol Vis Sci.* 2004;45:1404–1409.
22. Bland JM, Altman DG. Statistical methods for assessing agreement between two methods of clinical measurement. *Lancet.* 1986;1: 307–310.
23. Polito A, Del BM, Isola M, Zemella N, Bandello F. Repeatability and reproducibility of fast macular thickness mapping with stratus optical coherence tomography. *Arch Ophthalmol.* 2005;123: 1330–1337.
24. Patel PJ, Chen FK, Ikeji F, et al. Repeatability of stratus optical coherence tomography measures in neovascular age-related macular degeneration. *Invest Ophthalmol Vis Sci.* 2008;49:1084–1088.
25. Frenkel S, Morgan JE, Blumenthal EZ. Histological measurement of retinal nerve fibre layer thickness. *Eye.* 2005;19:491–498.
26. Hatton WJ, von Bartheld CS. Analysis of cell death in the trochlear nucleus of the chick embryo: calibration of the optical dissector counting method reveals systematic bias. *J Comp Neurol.* 1999; 409:169–186.
27. Budenz DL, Anderson DR, Varma R, et al. Determinants of normal retinal nerve fiber layer thickness measured by Stratus OCT. *Ophthalmology.* 2007;114:1046–1052.
28. Cohen MJ, Kaliner E, Frenkel S, Kogan M, Miron H, Blumenthal EZ. Morphometric analysis of human peripapillary retinal nerve fiber layer thickness. *Invest Ophthalmol Vis Sci.* 2008;49:941–944.
29. Fukuda Y. A three-group classification of rat retinal ganglion cells: histological and physiological studies. *Brain Res.* 1977;119:327–334.
30. Danias J, Shen F, Goldblum D, et al. Cytoarchitecture of the retinal ganglion cells in the rat. *Invest Ophthalmol Vis Sci.* 2002;43:587–594.
31. Villegas-Perez MP, Vidal-Sanz M, Rasminsky M, Bray GM, Aguayo AJ. Rapid and protracted phases of retinal ganglion cell loss follow axotomy in the optic nerve of adult rats. *J Neurobiol.* 1993;24:23–36.
32. Berkelaar M, Clarke DB, Wang YC, Bray GM, Aguayo AJ. Axotomy results in delayed death and apoptosis of retinal ganglion cells in adult rats. *J Neurosci.* 1994;14:4368–4374.
33. Gellrich NC, Schimming R, Zerfowski M, Eysel UT. Quantification of histological changes after calibrated crush of the intraorbital optic nerve in rats. *Br J Ophthalmol.* 2002;86:233–237.
34. Yoles E, Schwartz M. Degeneration of spared axons following partial white matter lesion: implications for optic nerve neuropathies. *Exp Neurol.* 1998;153:1–7.
35. Levkovitch-Verbin H, Quigley HA, Martin KRG, Zack DJ, Pease ME, Valenta DF. A model to study differences between primary and secondary degeneration of retinal ganglion cells in rats by partial optic nerve transaction. *Invest Ophthalmol Vis Sci.* 2003;44: 3388–3393.
36. DeLeón Ortega JE, Sakata LM, Kakati B, et al. Effect of glaucomatous damage on repeatability of confocal scanning laser ophthalmoscope, scanning laser polarimetry, and optical coherence tomography. *Invest Ophthalmol Vis Sci.* 2007;48:1156–1163.
37. Sander B, Larsen M, Thrane L, Hougaard JL, Jørgensen TM. Enhanced optical coherence tomography imaging by multiple scan averaging. *Br J Ophthalmol.* 2005;89:207–212.